ELSEVIER

Global and Planetary Change 35 (2002) 131–141

GLOBAL AND PLANETARY CHANGE

www.elsevier.com/locate/gloplacha

Carbon cycling and climate change during the last glacial cycle inferred from the isotope records using an ocean biogeochemical carbon cycle model

Takashi Ikeda*, Eiichi Tajika

Department of Earth and Planetary Science, Geological Institute School of Science, University of Tokyo, 7-3-1, Hongo, Bunkyo-ku, Tokyo, 113-0033, Japan

Accepted 1 March 2002

Abstract

We construct a simple, vertical one-dimensional ocean model coupled with carbon biogeochemical cycle model in order to study the carbon cycle in association with the glacial–interglacial cycle. The model is time-integrated by using the atmospheric CO_2 concentration and the marine carbon isotope record of the surface and the deep water during the last 130,000 years. Temporal variation of the mean upwelling rate, productivity of organic carbon, productivity of carbonate carbon, and the terrestrial carbon storage are obtained from the mass balances of the total carbon, the ^{13}C of dissolved inorganic carbon (DIC), the total alkalinity, and the dissolved phosphate. Variation of the terrestrial biomass size is similar to the $\delta^{18}O$ curve obtained from deep-sea sediments, suggesting that the terrestrial biomass change has been influenced by climate change. As far as we know, this is the first attempt to reconstruct the temporal variation of the terrestrial carbon storage during the last 130,000 years. The obtained terrestrial carbon storage at the last glacial maximum is within the range estimated in previous studies. Vertical mixing of the ocean is weakened and the bioproductivity decreases globally during the glacial intervals. Although the obtained variations of organic carbon and carbonate productivities are similar to each other, remarkable increases at the deglaciations are found only in carbonate productivity. The variation of nutrient concentration in the intermediate water differs from that in the deep water, while the variations of the total alkalinity in the intermediate and the deep water are in phase. The glacial ocean is characterized by higher alkalinity throughout the water column and lower gradient of DIC and nutrient. This lower gradient, resulting from lower upwelling rate and organic carbon productivity, results in a redistribution of DIC and nutrient between the intermediate and the deep water, but not change the total stock of DIC. On the other hand, higher alkalinity in the glacial intervals results in an increase in the total stock of dissolved inorganic carbon in the ocean because of increased solubility of atmospheric CO_2 from higher alkalinity throughout the water column. Temporal variations in alkalinity are characterized by abrupt decreases corresponding to the deglaciations every 100,000 years, resulting from a remarkable increase in carbonate productivity. This might indicate a relationship with the variation of atmospheric CO_2 level, which shows a gradual decrease through the glacial interval and an abrupt increase at the deglaciations. Higher alkalinity in the glacial intervals would be a result of an integral effect of the lower net carbonate burial rate during those periods. On the other hand, the redistribution of nutrients and dissolved carbon between the intermediate and the deep water shows shorter-term fluctuations. This would not change the atmospheric CO_2 level significantly, probably because the integral effect of net

* Corresponding author. Tel.: +81-3-5841-4538; fax: +81-3-3815-9490.
E-mail addresses: ikd@sys.eps.s.u-tokyo.ac.jp (T. Ikeda), tajika@eps.s.u-tokyo.ac.jp (E. Tajika).

0921-8181/02/$ - see front matter
PII: S0921-8181(02)00134-0

carbonate burial may not be enough to change the total alkalinity over the water column.

Keywords: carbon cycle; glacial–interglacial cycle; deglaciation; terrestrial biomass; carbon isotope

1. Introduction

Carbon cycling within the Earth's surface system plays an important role in climate change through controlling the atmospheric CO_2 level. Exchange of atmospheric CO_2 using the surface ocean and biosphere is the dominant controlling mechanism for the atmospheric CO_2 level on short time scales ($<10^2$ years) (Oeschger et al., 1975; Siegenthaler and Oeschger, 1978; Bolin et al., 1981), while silicate weathering and burial of biogenic particles into the seafloor sediments are dominant on longer time scales ($>10^6$ years) (Walker et al., 1981; Berner et al., 1983; Berner, 1997; Tajika, 1998). These problems have been studied quantitatively by using numerical models, such as general circulation models (Heinze et al., 1991; Yamanaka and Tajika, 1996) and box-models (e.g. Berger and Keir, 1984; Knox and McElroy, 1984; Sarmiento and Toggweiler, 1984; Siegenthaler and Wenk, 1984). However, although the atmospheric CO_2 level also changed during the glacial–interglacial cycles (Jouzel et al., 1993), there is no established numerical model which can analyze the temporal variation of carbon cycle system in such an intermediate time-scale (10^3–10^5 years). This might be partly because the model for such an intermediate time-scale should consider the processes of carbon cycle both for the short time-scales and the long time-scales. Although geological records such as $\delta^{13}C$ of foraminifers have potential information for reconstructing these changes, most of previous studies on carbon isotope data seem to be limited to providing qualitative discussion.

There may be various fluctuations related to the carbon cycle during the glacial–interglacial cycle. The most prominent variation during the glacial–interglacial cycle would be the variation of atmospheric CO_2 concentration, which is characterized by a gradual decrease through the glacial period and an abrupt increase corresponding to deglaciations, with about 100 ka periodicity (Jouzel et al., 1993). This might be the most typical climatic variation for the glacial–interglacial cycle, as suggested by marine $\delta^{18}O$ record in most of major areas in the world ocean. On the other hand, short time-scale variations ($\sim$ 20 ka) seem to be prominent in the $\delta^{13}C$ records of planktonic and benthic foraminifers, and much shorter time-scale variations, such as Dansgaard–Oeschger cycles, have been found during the glacial period (Dansgaard et al., 1984; Oeschger et al., 1984). However, variations of marine chemistry and processes for the carbon cycle during these time-scales have not been well studied using numerical models.

In this study, we try to develop a simple, numerical model of the carbon cycle during the last glacial cycle based on physical and biogeochemical processes within the ocean combined with the carbon isotope record, and to reconstruct the temporal variations of various processes that might have affected the carbon cycle during the last 130,000 years. Variations of marine chemistry corresponding to the fluctuations seen in the glacial–interglacial cycle will be also discussed.

2. Model and methods

We constructed a simple, vertical 11-layered one-dimensional ocean model which includes diffusive and advective transport of dissolved materials, dissolution equilibrium with atmospheric CO_2, bioproduction of particulate carbonate and organic matter in the surface ocean, regeneration of organic matter and dissolution of biogenic carbonate in the deep ocean, and carbon isotope fractionation in each process (Fig. 1). We treat the total dissolved inorganic carbon ($[\Sigma CO_2]$), the ^{13}C in total dissolved inorganic carbon ($[\Sigma^{13}CO_2]$), the total alkalinity ($[Alk_T]$), and dissolved phosphate ($[PO_4]$).

A one-dimensional ocean model might be too simple to represent the world ocean, because marine chemistry ($[\Sigma CO_2]$, $[\Sigma^{13}CO_2]$, $[Alk_T]$, and $[PO_4]$) is

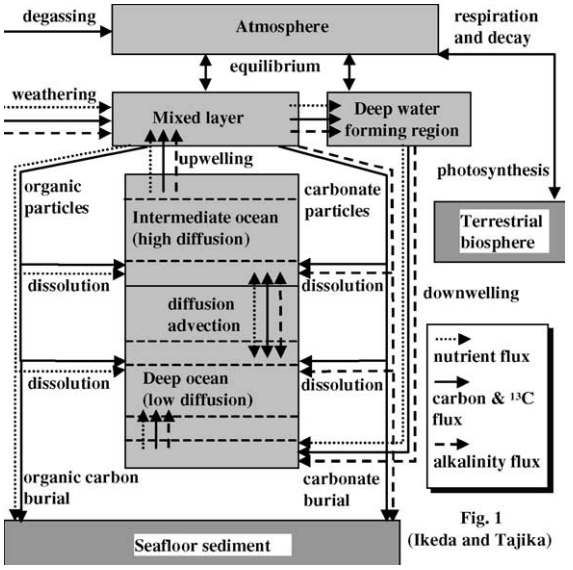

Fig. 1. Schematic illustration of the carbon cycle model used in this study.

different in regions owing to accumulation of the light carbon through the horizontal transport of deep water masses and regional difference in the temperature fields. However, such a model might be useful to investigate the global trend of variations in the carbon cycle system, because the patterns of the temporal variations of $\delta^{13}C$ in the surface and the deep oceans are similar in most of the major areas in the world ocean in time-scales of longer than thousands of years.

Mass balance equation in each layer of the ocean except the ocean mixed layer is

$$\frac{\partial C^x}{\partial t} = W\frac{\partial f_w C^x}{\partial z} - W\frac{\partial f_w}{\partial z}C^x_m + \frac{\partial}{\partial z}\left(K(z)\frac{\partial C^x}{\partial z}\right) - q^x_c\frac{\partial f_c}{\partial z}P_c - q^x_o\frac{\partial f_o}{\partial z}P_o \quad (1)$$

where z is the water depth, $K(z)$ is diffusion coefficient, C^x is the concentration of each component x ($[\Sigma CO_2]$, $[\Sigma^{13}CO_2]$, $[Alk_T]$, and $[PO_4]$), C^x_m is the concentration of each component x in the ocean mixed layer, W is the global mean upwelling rate, f_w is the vertical profile of upwelling (0 at the sea bottom and 1 for other depth), f_c and f_o are the vertical profiles of the vertical fluxes of carbonate carbon and organic matter (Yamanaka and Tajika, 1996), P_c and P_o are the export production of particulate carbonate and organic carbon, and q^x_c and q^x_o are the coefficients for dissolution of each tracer in biogenic particles (Table 1).

Mass balance equation in the ocean mixed layer is

$$h_m\frac{\partial C^x}{\partial t} = -WC^x_m + WC^x(z=h_m) + K(h_m)\left.\frac{\partial C^x}{\partial z}\right|_{z=h_m} - q^x_cP_c - q^x_oP_o + F^x_l/A + F^x/A \quad (2)$$

where h_m is the depth of ocean mixed layer, and A is the area of model ocean. F^x_l is the net input flux from the terrestrial biosphere to the ocean–atmosphere system via photosynthesis and decomposition. The relationships between F^x_l are

$$F^{[\Sigma^{13}CO_2]}_l = \delta_l F^{[\Sigma CO_2]}_l \quad (3)$$

$$F^{[Alk]}_l = 0 \quad (4)$$

$$F^{[PO_4]}_l = q_l F^{[\Sigma CO_2]}_l \quad (5)$$

where δ_l is the carbon isotope fractionation due to photosysthesis of the terrestrial biosphere and q_l is the P/C ratio for the terrestrial biosphere. F^x is the input flux of each component x to the ocean–atmosphere system due to weathering of continental silicate rocks and weathering and metamorphism of carbonate and organic carbon (Berner, 1991). Values for the parameters used at the control case are listed in Table 2. It should be noted that $C^{[\Sigma^{13}CO_2]}$ is defined here as $\delta^{13}C \times C^{[\Sigma CO_2]}$.

In addition, we consider the output flux due to burial of carbonate and organic carbon into seafloor sediments. The ocean mixed layer is assumed to be in dissolution equilibria with the atmosphere for $[\Sigma CO_2]$ (Edmond and Gieskes, 1970) and $[\Sigma^{13}CO_2]$ (Yamanaka and Tajika, 1996). The simple geometry of deep water circulation, downwelling in the high-latitude

Table 1
Coefficients for dissolution of each tracers from biogenic particles

x	$[\Sigma CO_2]$	$[\Sigma^{13}CO_2]$	[Alk]	$[PO_4]$
q^x_c	1	δ_s	2	0
q^x_o	1	$\delta_s - \alpha_{org}$	q_c	q_m

The δ_s, α_{org}, q_m represent the $\delta^{13}C$ value in the surface water, the fractionation via photosynthesis (Berner, 1991), and the Redfield Ratio (Redfield et al., 1963), respectively.

Table 2
Values for the parameters used in this study

Parameter	Value	Citation
K ($z<400$ m)	8000 m^2/year	This study
K (400 m$<z$)	2000 m^2/year	Wigley and Raper (1987)
h_m	75 m	Bolin et al. (1981)
α_{org}	21.8‰	Berner (1991)
δ_l	−25‰	Crowley (1995)
q_c	−16/106	Redfield et al. (1963)
q_m	1/106	Redfield et al. (1963)
q_l	1/800	Jahnke (1992)
$F^{[\Sigma CO_2]}$	2.5×10^{13} mol/year	Berner (1991)
$F^{[\Sigma^{13}CO_2]}$	-8.75×10^{13} mol/year	Berner (1991)
$F^{[Alk]}$	4.0×10^{13} mol/year	Berner (1991)
$F^{[PO_4]}$	6.05×10^{10} mol/year	This study

and upwelling in the middle-to-low latitude, is assumed in the model. Although the deep water circulation pattern might have changed during the glacial–interglacial cycle, this assumption might be a first approximation because lower circulation rate would be almost equivalent to the shallower ventilation for the $\delta^{13}C$ in surface, intermediate, and deep water in this model. Deep water forming region is separated from the rest of the ocean in order to adopt lower sea surface temperature for dissolution equilibria with the atmosphere. The schematic illustration of the model is shown in Fig. 1.

We use some geological information from the last 130,000 years as boundary conditions of the model (Fig. 2): (1) variation of atmospheric CO_2 concentration estimated from Vostok ice cores (Jouzel et al., 1993), (2) variation of $\delta^{13}C$ of surface water estimated from planktonic foraminifers (Mulitza et al., 1998), and (3) variation of $\delta^{13}C$ of bottom water estimated from benthic foraminifers (Mulitza et al., 1998). Because this model is one-dimensional, we should adopt the global mean $\delta^{13}C$ data for the surface and bottom waters to the boundary conditions of the model. In this study, however, we adopt the $\delta^{13}C$ data obtained from the deep-sea sediments at the equatorial Atlantic core GeoB 1523-1 (Mulitza et al., 1998) and the equatorial Pacific (Shackleton and Pisias, 1985) separately. Although the Atlantic Ocean occupies only a quarter of the whole ocean, the patterns of the temporal variations of $\delta^{13}C$ in the surface ocean and the deep ocean are similar to those for most of the major areas in the world ocean. In the Pacific, the amplitude of $\delta^{13}C$ is less than that in the Atlantic, but the pattern of the variation is very similar. We calculated the model with the $\delta^{13}C$ record of the Pacific Ocean and found that, although amplitudes of variations are smaller, the patterns of variations are very similar to those obtained from the model with the $\delta^{13}C$ record of the Atlantic. Therefore, we will show the results only for the Atlantic case in this paper. This could be regarded as a first approximation of the world ocean variations, although the amplitudes of variations might be larger than those for the average of world oceans.

The model equations are time-integrated with the boundary conditions of the time series of geological data described above. Global mean upwelling rate, productivity of organic carbon, productivity of carbonate carbon, and the size of terrestrial biosphere are predicted internally. Among these, productivity of organic carbon is determined corresponding to nutrient supply into the ocean mixed layer (Yamanaka and Tajika, 1996), while global mean upwelling rate, productivity of carbonate carbon, and the size of terrestrial biosphere are determined by the mass balance of $[\Sigma CO_2]$, $[\Sigma^{13}CO_2]$, and $[Alk_T]$. Note that carbonate productivity and organic carbon productivity are determined independently in the model. The initial conditions and parameters are given by the values of observed $[\Sigma CO_2]$, $[Alk_T]$, and $\delta^{13}C$ of the

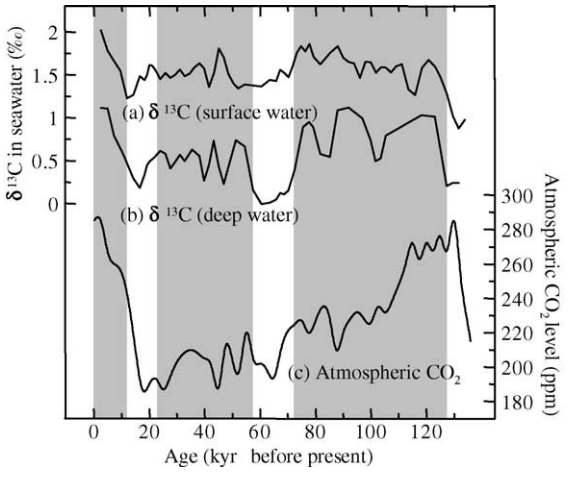

Fig. 2. Input data used in this study. (a) $\delta^{13}C$ in the ocean mixed layer (Mulitza et al., 1998); (b) $\delta^{13}C$ in the bottom ocean (Mulitza et al., 1998); and (c) atmospheric CO_2 partial pressure (Jouzel et al., 1993).

surface and bottom water at present (Broecker and Peng, 1982), and the model is integrated for several tens thousands years before 130 ka BP to avoid influences of initial conditions.

3. Numerical results

Fig. 3 shows the numerical results of temporal variations of (a) organic carbon productivity, (b) carbonate carbon productivity, (c) global mean upwelling rate, and (d) size of terrestrial biosphere (difference in the terrestrial carbon storage from the pre-industrial value). Note that productivities of carbonate and organic carbon represent the export production at 100-m water depth.

The temporal variation of the terrestrial biomass suggests that the terrestrial carbon storage would have been reduced under cold climates, such as the marine isotope stages (MIS) 2 and 4 (Fig. 3d). The estimated value for the last glacial maximum (LGM) is about 630 GtC smaller than that at present, which is consistent with the range estimated from reconstruction of the global vegetation at that time (Crowley, 1995; Franc,ois et al., 1998; see Fig. 3d).

Global mean upwelling rate defined in this model would be regarded as the strength of deep water circulation. The result indicates that the deep water circulation would have been weaker during the cold stages (stages 2 and 4) and the cold substages within the stage 5 (Fig. 3c). Change in the circulation rate affects the distribution of nutrients between the intermediate and the deep water. As a result, the deep water would have been richer in nutrient during cold stages. Fig. 5a illustrates the results of vertical profiles of $[PO_4]$ within the ocean at the stage 4, the LGM, and the Holocene. Some geological evidences suggest that the deep water would have been richer in nutrients at the LGM (Oppo and Fairbanks, 1990; Beveridge et al., 1995). However, the characteristics of the glacial ocean (nutrient richer in the deep water as a result of lower circulation rate) is clearly seen at the stage 4 and, to a lesser extent, at the LGM (Figs. 3 and 5a). At the LGM, not only the deep water but also the intermediate water would have been richer in nutrient. This is because the nutrient influx to the ocean would have increased at the LGM due to the reduced terrestrial biosphere at this time.

Temporal variations of the reconstructed productivities of carbonate and organic carbon are similar to each other except for the MIS 5 and 6, although these quantities are calculated independently. However, it should be noted that only the carbonate productivity shows remarkable increases at the deglaciations (18 and 130 ka BP). The results imply that decreased deep water circulation results in less organic carbon productivity due to less nutrient supply to the ocean mixed layer during the cold stages (stages 2 and 4) and in the cold substages within the stage 5. Some previous studies suggest higher organic carbon productivity in the equatorial Pacific during the glacial

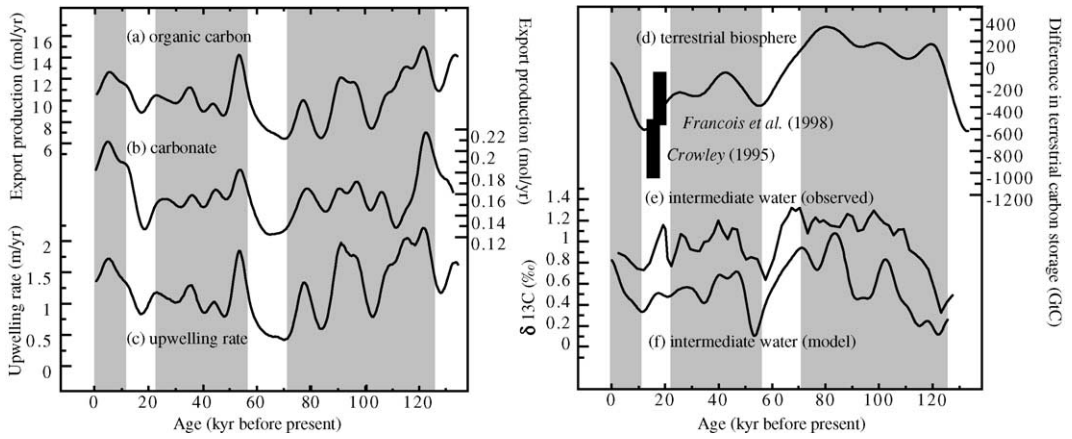

Fig. 3. The model results. (a) Organic carbon productivity, (b) carbonate productivity, (c) global mean upwelling rate, (d) difference in the terrestrial carbon storage from the present-day amount (hatched area represents the estimate by Crowley (1995), (e) observed $\delta^{13}C$ in deep dwelling foraminifer, *G. truncatulinoides* (Mulitza et al., 1998), (f) calculated $\delta^{13}C$ in 100 m depth.

periods (e.g. Farrell et al., 1995), and the variation of non-seasalt sulphate profile obtained from the Vostok ice-core indicates larger dimethyl sulfide emission from the marine biosphere, which implies world-wide increase in marine bioproductivity (Legrand et al., 1988). Although it remains unknown whether organic carbon productivity during the glacial periods was larger not only in some restricted areas but also in the global ocean (Crowley and North, 1995), the model result might be somewhat controversial. Reduced terrestrial biosphere could have resulted in an increase of the nutrient supply to the ocean, and thus organic carbon productivity. However, this effect would not be sufficient because the C/P ratio of the terrestrial biosphere is usually greater than that of marine biosphere (that is, Redfield ratio) (Jahnke, 1992). If the global organic carbon productivity were really large, it might be because the nutrient utilization in the ocean as a whole would have been higher in glacial stages for some reason (e.g. Martin, 1990).

The $\delta^{13}C$ value in deep dwelling planktonic foraminifer *Globorotalia truncatulinoides*, which may record the change of intermediate water chemistry, is also measured in the same core from which we adopted the $\delta^{13}C$ values for the surface and the deep waters (Mulitza et al., 1998). The temporal variation of $\delta^{13}C$ in 100 m water depth calculated in this model (Fig. 3e) is compared with the $\delta^{13}C$ value from *G. truncatulinoides* (Fig. 3f). Although the isotope fractionation of *G. truncatulinoides* is not well known, the pattern of the variation would reflect the variation of the $\delta^{13}C$ value in the intermediate water. The result seems to be roughly consistent with the observation. The temporal variation of the intermediate water $\delta^{13}C$ shows the higher values in the cold stages and lower values at the transition from the cold to the warm stages. This trend is quite opposite to the $\delta^{13}C$ variation in the deep water. This is caused mainly by the nutrient redistribution between the intermediate and the deep water and change in the supply of the light carbon from the terrestrial biosphere to the ocean. The agreement of the calculated $\delta^{13}C$ variation of the intermediate water with the observation may support the validity of the results for the variations of the deep water circulation rate and the terrestrial biomass.

We assumed the fixed reverline silicate weathering flux in our model. However, it may be climatically controlled during the glacial–interglacial cycles (Froelich et al., 1992; Gibbs and Kump, 1994). We therefore made a sensitivity test (Fig. 4), in which reverline silicate weathering fluxes vary in proportion to the seawater $\delta^{18}O$ variation. The results indicate that higher weathering flux at the cold stages reduces the amplitude of the variation in bioproductivity, although its pattern does not change greatly. Therefore, if reverline silicate flux was really higher at the LGM (Gibbs and Kump, 1994; Munhoven and François 1996), the control case would overestimate change in the bioproductivity. In this respect, our results can be regarded as a maximum estimate of change in the bioproductivity during the glacial–interglacial cycles.

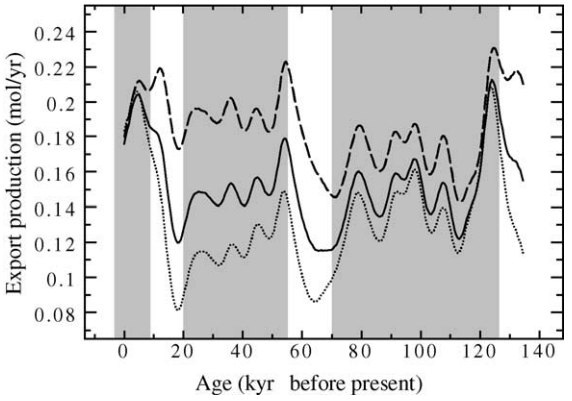

Fig. 4. Sensivity test for effect of change in the continental silicate weathering flux. Solid, dashed, and dotted curve represent the carbonate productivity in the cases of silicate weathering flux to be constant, 50% higher at the LGM, and 50% lower at the LGM, respectively.

4. Atmospheric CO_2 variability

Atmospheric CO_2 level is estimated to be about 80 ppm lower at the LGM than that of preceding anthropogenic perturbation (Jouzel et al., 1993). One of the main interests concerning the carbon cycle during the glacial–interglacial cycle would be the cause for the atmospheric CO_2 variability. The ocean is believed to have played an important role in determining past atmospheric CO_2 level (Broecker and Peng, 1982). The vertical one-dimensional model used in this study might be too simple to clarify the change of the past atmospheric CO_2 level, because the atmospheric CO_2 level of 80 ppm corresponds to only 0.5% of the total

dissolved carbon in the ocean, and so regional changes, such as the change in the Southern Ocean outcrops of CO_2 (e.g. François et al., 1997), could have been as important as global change. However, the vertical profile of the marine chemistry obtained from the model may provide some important implications.

Fig. 5b and c illustrates the results of vertical profiles of $[\Sigma CO_2]$ and $[Alk_T]$, respectively, within the ocean at the stage 4, the LGM, and the Holocene. The vertical $[\Sigma CO_2]$ profile (Fig. 5b) indicates that the total stock of the dissolved CO_2 would have increased at the cold stages (the LGM and the stage 4). The change in the dissolved CO_2 in the glacial ocean relates with two factors: one is the lower gradient of $[\Sigma CO_2]$, which resulted in the redistribution of the dissolved CO_2 between the intermediate and the deep water; and another is the increased atmospheric CO_2 solubility (increased $[\Sigma CO_2]$ at the top of the ocean mixed layer). The former does not change the total stock of dissolved inorganic carbon in the ocean. This could be understood as follows: lower deep water circulation rate in the glacial intervals would increase residence time of the deep water, resulting in lower atmospheric CO_2, while lower organic carbon productivity would have resulted in higher atmospheric CO_2, and so these effects would be canceled out, although both would result in the $[\Sigma CO_2]$ redistribution between the intermediate and the deep water. However, increased $[\Sigma CO_2]$ at the top of the ocean mixed layer results in change in the total stock of dissolved inorganic carbon in the ocean. This results from the increased alkalinity at the ocean–atmosphere boundary, corresponding to an increase in alkalinity over the water column in the ocean (Fig. 5c). The increased alkalinity over the water column is achieved in this model by the integral effect of lower rate of net carbonate burial due to decreased carbonate productivity in the cold stages (Fig. 3b).

Nutrient redistribution between the intermediate and the deep water during the glacial stages might also result in an increase in the alkalinity due to carbonate dissolution owing to change in sedimentary calcite preservation (Boyle, 1988a), which is not expressed directly in this model. As described above, the model result indicates the nutrient redistribution between the intermediate and the deep water, which implies that carbonate dissolution would be accelerated in the cold stages (Boyle, 1988b). Carbonate productivity is estimated here as a net burial of carbonate constrained from the surface and the deep water $\delta^{13}C$ values. Therefore, the obtained amplitude of the carbonate productivity might be too large. However, the pattern of the model result of the carbonate productivity should be consistent with the net burial flux of carbonate into the seafloor.

5. Abrupt change in marine chemistry during the last glacial cycle

Fig. 6 shows the temporal variations of the vertical profiles of (a) the dissolved phosphate concentration ($[PO_4]$), (b) the total dissolved inorganic carbon

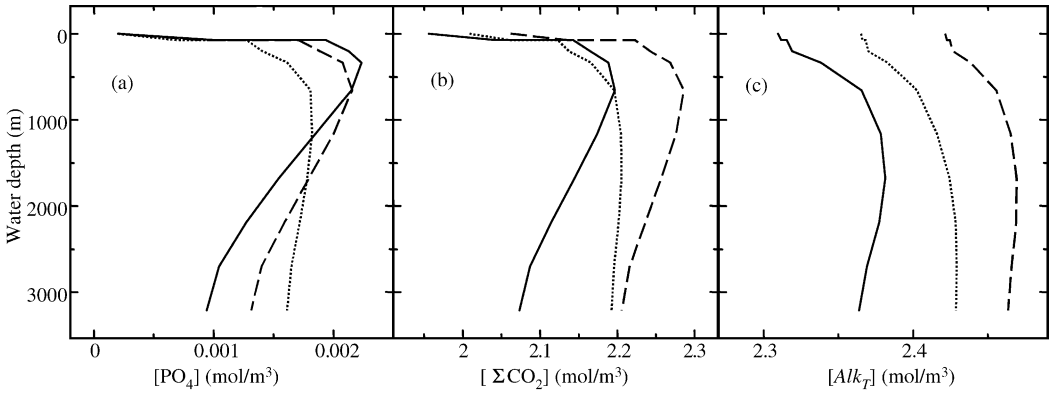

Fig. 5. Vertical profiles of (a) dissolved phosphate ($[PO_4]$), (b) total dissolved inorganic carbon ($[\Sigma CO_2]$), and (c) total alkalinity ($[Alk_T]$) in the ocean at the stage 4 (dotted line), at the LGM (dashed line), and at the Holocene (solid line).

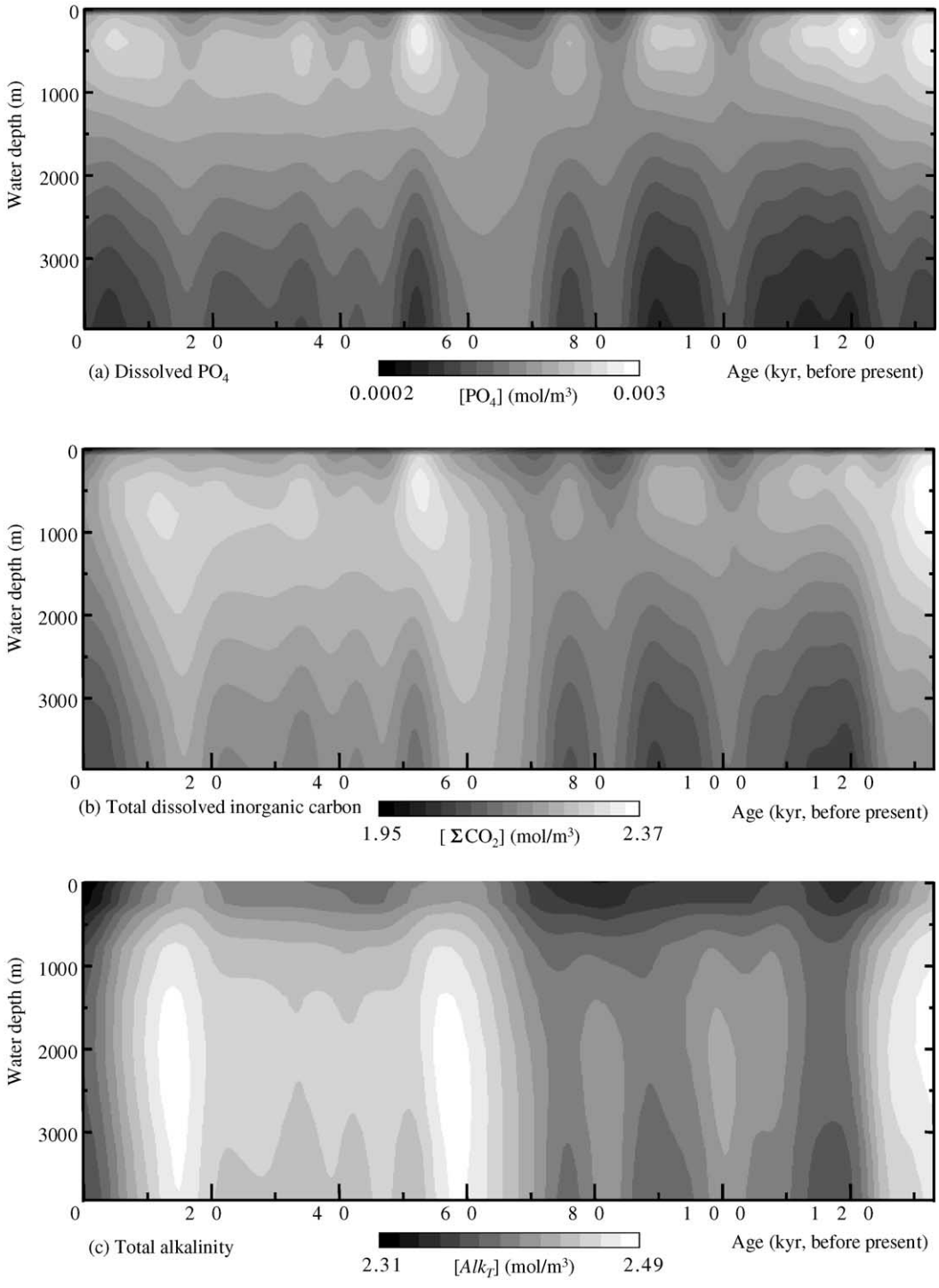

Fig. 6. Vertical profiles of (a) dissolved phosphate ([PO_4]), (b) total dissolved inorganic carbon ([ΣCO_2]), and (c) total alkalinity ([Alk_T]) in the ocean during the last 130,000 years.

([ΣCO_2]), and (c) the total alkalinity ([Alk_T]) during the last 130,000 years, respectively.

The temporal variation of the dissolved phosphate concentration (Fig. 6a) is characterized by short-term fluctuations which correspond to the $\delta^{13}C$ variation in the surface and the deep water. As described above, this would be attributed to change in the deep water circulation rate and the productivity of organic carbon. Therefore, the phase relationship between the intermediate and the deep water is opposite for the dissolved phosphate and the $\delta^{13}C$. On the other hand, the temporal variation of the total alkalinity (Fig. 6c) is characterized by abrupt decreases corresponding to the deglaciations (after 18 and 130 ka BP). Abrupt decrease in the total alkalinity is seen every 100 ka during the glacial cycle, but the short-term fluctuation is not clearly seen. The variation is found to be in the same phase throughout the water column. Note that the signal for the abrupt change at the deglaciations is not found in the [PO_4] variation. The conspicuous increase in alkalinity during the stage 4 (60–70 ka) might be attributed to the low net carbonate burial rate, possibly due to the dissolution of sedimentary calcite corresponding to the very low upwelling rate. In fact, Mulitza et al. (1998) reported a low carbonate accumulation rate and high foraminiferal fragmentation during this interval. The temporal variation of the total dissolved inorganic carbon (Fig. 6b) is affected by redistribution between the intermediate and the deep water and also by change in solubility of CO_2 due to change in the alkalinity over the water column. Therefore, the variation of the total dissolved inorganic carbon shows these two features: abrupt decreases over the water column at the deglaciations, and the redistribution of [ΣCO_2] between the intermediate and the deep water.

Atmospheric CO_2 variation (Fig. 2c) shows an abrupt increase at the deglaciations. This would correspond to the abrupt decrease in the [ΣCO_2] throughout the water column at these times (Fig. 6). This implies that the variation of atmospheric CO_2 might be controlled by change in the total alkalinity of the ocean. The abrupt decrease in the total alkalinity in the ocean at the deglaciations might have related with the higher rate of net carbonate burial at the deglaciation (Fig. 3b). On the other hand, the short-term fluctuation found in marine $\delta^{13}C$ records would reflect the change in deep water circulation and productivity of organic carbon (Fig. 3a and c), which would have influenced the distribution of [PO_4] and [ΣCO_2] between the intermediate and the deep water, but not the alkalinity over the water column, and thus the atmospheric CO_2 change.

Recent studies on Greenland ice cores indicate much shorter-term fluctuation of atmospheric temperature over Greenland during the glacial intervals, called Dansgaard–Oeschger oscillation (Grootes et al., 1992). This might be related to the freshwater inflow to the North Atlantic (Heinrich, 1988) resulting in a change in deep water production rate (Broecker et al., 1990). Although its climatic impact might compare with the glacial–interglacial variation (Taylor et al., 1993), the simultaneous variation of the atmospheric CO_2 is not clearly seen in the ice core record. It is suggested that this might be because the atmospheric CO_2 would not depend strongly on the deep water circulation rate as described above, although such millennium scale fluctuations could not detected in this study because millennium scale variations are not found in the input data used in the model. Change in the total alkalinity over the water column is a result of the integral effect of change in the net carbonate burial through the time. The millennium scale oscillation might be too short to cause the alkalinity change significantly over the water column, even if the carbonate productivity might have changed in this time-scale.

6. Summary

We developed a carbon cycle model with a vertical one-dimensional ocean and tried to reconstruct temporal variations of deep water circulation rate, bioproductivities of organic carbon and carbonate carbon, and the size of terrestrial biomass, using the atmospheric CO_2 variations and the carbon isotope record of the surface and the deep water during the last 130,000 years. Results and implications are as follows.

(1) The temporal variation of the carbon storage in the terrestrial biosphere reconstructed from this model suggests that the terrestrial biosphere would have been reduced under the cold climate (the oxygen isotope stages 2 and 4). The estimated value for the LGM is consistent with the estimated ranges obtained from the previous studies.

(2) During the cold stages (stages 2 and 4) and the cold substages within the stage 5, the deep water circulation rate would have been lower and the productivity of organic carbon would also have been lower. Both factors would have resulted in the redistribution of nutrient and [ΣCO_2] between the intermediate and the deep water.

(3) The calculated $\delta^{13}C$ variation at the 100 m water depth of the ocean seems to be roughly consistent with the observed $\delta^{13}C$ variation of intermediate water.

(4) The temporal variations of productivity of carbonate are similar to that of organic carbon, but the remarkable changes at the deglaciations are found only in carbonate productivity.

(5) The atmospheric CO_2 level was lower during the glacial period probably because the ocean would have stocked much carbon due to the increase in alkalinity over the water column. This would be attributed to the integral effect of the lower rate of net carbonate burial during the glacial period.

(6) Change in the alkalinity over the water column is characterized by the abrupt decrease corresponding to the deglaciations in every 100 ka, while the redistribution of nutrient and dissolved carbon between intermediate and deep water shows shorter-term fluctuations.

Acknowledgements

We thank Dr. N. Ohkouchi and Dr. L.R. Kump for their critical reviews and helpful comments. We also thank to R. Tada for his helpful comments. This research was partially supported by Research Fellowships of the Japan Society for the Promotion of Science for Young Scientist and the grants-in-aid for Scientific Research (No. 09740363) of the Ministry of Education of Japan.

References

Berger, W.H., Keir, R.S., 1984. Glacial-Holocene changes in atmospheric CO_2 and the deep-sea record. In: Hansen, J.E., Takahashi, T. (Eds.), Climate Processes and Climate Sensitivity. AGU, Washington, DC, pp. 337–351.

Berner, R.A., 1991. A model for atmospheric CO_2 over Phanerozoic time. American Journal of Science 291, 339–376.

Berner, R.A., 1997. The rise of plants and their effect on weathering and atmospheric CO_2. Science 276, 544–546.

Berner, R.A., Lasaga, A.C., Garrels, R.M., 1983. The carbonate–silicate geochemical cycle and its effect on atmospheric carbon dioxide over the past 100 million years. American Journal of Science 283, 641–683.

Beveridge, A.A.S., Elderfield, H., Shackleton, N.J., 1995. Deep thermohaline circulation in the low-latitude Atlantic during the last glacial. Paleoceanography 10, 643–660.

Bolin, B., Björkström, A., Keeling, C.D., Bacastow, R., Siegenthaler, U., 1981. Carbon cycle modeling. In: Bolin, B. (Ed.), Carbon Cycle Modeling. SCOPE, vol. 16. Wiley, New York, pp. 1–28.

Boyle, E.A., 1988a. Vertical oceanic nutrient fractionation and glacial/interglacial CO_2 cycles. Nature 331, 55–56.

Boyle, E.A., 1988b. The role of vertical chemical fractionation in controlling late Quaternary atmospheric carbon dioxide. Journal of Geophysical Research, 93 (15) 701–15, 714.

Broecker, W.S., Peng, T.-H., 1982. Tracers in the seaLamont-Doherty Geological Observatory. Columbia Univ., Palisades, NY, 690 pp.

Broecker, W.S., Bond, G., Klas, M., Bonani, G., Wolfli, W., 1990. A salt oscillator in the glacial Atlantic? 1. The concept. Paleoceanography 5, 469–477.

Crowley, T.J., 1995. Ice age terrestrial carbon changes revisited. Global Biogeochemical Cycles 9, 377–389.

Crowley, T.J., North, G.R., 1995. Paleoclimatology Oxford Univ. Press, New York, 349 pp.

Dansgaard, W., Johnsen, S.J., Clausen, H.B., Dahl-Jensen, D., Gundstrup, N., Hammer, C.U., Oeschger, H., 1984. North Atlantic climatic oscillations revealed by deep Greenland ice cores. In: Hansen, J.E., Takahashi, T. (Eds.), Climate Processes and Climate Sensitivity. American Geophysical Union, Washington, DC, pp. 288–298.

Edmond, J.M., Gieskes, J.M.T.M., 1970. On the calculation of the degree of saturation of sea water with respect to calcium carbonate under in situ condition. Geochemistry et Cosmochemistry Acta 34, 1261–1291.

Farrell, J.W., Pedersen, T.F., Nielsen, B., 1995. Glacial–interglacial changes in nutrient utilization in the equatorial Pacific Ocean. Nature 377, 514.

François, R., Altabet, M.A., Yu, E.-F., Sigman, D.M., Bacon, M.P., Frank, M., Bohrmann, G., Bareille, G., Labeyrie, L.D., 1997. Contribution of Southern Ocean surface-water stratification to low atmospheric CO_2 concentrations during the last glacial period. Nature 389, 929–935.

François, L.N., Delire, C., Warnant, P., Munhoven, G., 1998. Modeling the glacial–interglacial changes in the continental biosphere. Global and Planetary Change 16–17, 37–52.

Froelich, P.N., Blanc, V., Mortlock, R.A., Chillrud, S.N., 1992. River fluxes of dissolved silica to the ocean were higher during glacials: Ge/Si in diatoms, rivers, and oceans. Paleoceanography 7, 739–767.

Gibbs, M.T., Kump, L.R., 1994. Global chemical erosion during the last glacial maximum and the present: sensitivity to changes in lithology and hydrology. Paleoceanography 9, 529–543.

Grootes, P.M., Stuiver, M., White, J.W.C., 1992. Comparison of oxygen isotope records from the GISP2 and GRIP Greenland ice cores. Nature 266, 552.

Heinrich, H., 1988. Origin and consequences of cyclic ice rafting in the Northeast Atlantic Ocean during the past 130,000 years. Quaternary Research 29, 143–152.

Heinze, C., Maier-Reimer, E., Winn, K., 1991. Global pCO_2 reduction by the world ocean: experiments with the Hamburg Carbon Cycle Model. Paleoceanography 6, 395–430.

Jahnke, R.A., 1992. The phosphorus cycle. Global Biogeochemical Cycles. Academic Press, pp. 301–315.

Jouzel, J., Barkov, N.I., Barnola, J.M., Bender, M., Chappellaz, J., Genthon, C., Kotlyakov, V.M., Lipenkov, V., Lourius, C., Petit, J.R., Raynaud, D., Reisbeck, G., Ritz, C., Sowers, T., Stievenard, M., Yiou, F., Yiou, P., 1993. Extending the Vostok ice-core record of paleoclimate to the penultimate glacial period. Nature 364, 407–412.

Knox, F., McElroy, M.B., 1984. Changes in atmospheric CO_2: influence of the marine biota at high latitude. Journal of Geophysical Research 89 (D3), 4629–4637.

Legrand, M.R., Delmas, R.J., Charlson, R.J., 1988. Climate forcing implications from Vostok ice-core sulphate data. Nature 334, 418–420.

Martin, J.H., 1990. Glacial–interglacial CO_2 change: the iron hypothesis. Paleoceanography 5, 1–13.

Mulitza, S., Rühlemann, C., Bickert, T., Hale, W., Pätzold, J., Wefer, G., 1998. Late Quaternary $\delta^{13}C$ gradients and carbonate accumulation in the western equatorial Atlantic. Earth and Planetary Science Letters 155, 237–249.

Munhoven, G., François, L.M., 1996. Glacial–interglacial variability of atmospheric CO_2 due to changing continental silicate rock weathering: a model study. Journal of Geophysical Research 101, 21423–21437.

Oeschger, H., Siegenthaler, U., Schotterer, U., Gugelman, A., 1975. A box diffusion model to study the carbon dioxide exchange in nature. Tellus 27, 168–192.

Oeschger, H., Beer, J., Siegenthaler, U., Stauffer, B., Dansgaard, W., Langway, C.C., 1984. Late glacial history from ice cores. In: Hansen, J.E., Takahashi, T. (Eds.), Climate Processes and Climate Sensitivity. American Geophysical Union, Washington, DC, pp. 299–306.

Oppo, D.W., Fairbanks, R.G., 1990. Atlantic ocean thermohaline circulation of the last 150,000 years: relationship to climate and atmospheric CO_2. Paleoceanography 5, 277–288.

Redfield, A.C., Ketchum, B.H., Richards, F.A., 1963. The influence of organisms on the composition of sea-water. The Sea 2, 26–87.

Sarmiento, J.L., Toggweiler, J.R., 1984. A new model for the rol of the ocean in determining atmospheric p_{CO_2}. Nature 308, 621–624.

Siegenthaler, U., Oeschger, H., 1978. Predicting future atmospheric carbon dioxide levels. Science 199, 388–395.

Siegenthaler, U., Wenk, T., 1984. Rapid atmospheric CO_2 variations and ocean circulation. Nature 308, 624–626.

Shackleton, N.J., Pisias, N.G., 1985. Atmospheric carbon dioxide, orbital forcing, and climate. In: Sundquist, E.T., Broecker, W.S. (Eds.), The Carbon Cycle and Atmospheric CO_2: Natural Variations Archean to Present. Geophysical Monograph Series, vol. 32. AGU, Washington, DC, pp. 303–317.

Tajika, E., 1998. Climate change during the last 150 million years: reconstruction from a carbon cycle model. Earth and Planetary Science Letters 160, 695–707.

Taylor, K.C., Lamoray, G.W., Doyle, G.A., Alley, R.B., Grootes, P.M., Mayewski, P.A., White, J.W.C., Barlow, L.K., 1993. The 'flickering switch' of late Pleistocene climate change. Nature 361, 432–436.

Walker, J.C.G., Hays, P.B., Kasting, J.F., 1981. A negative feedback mechanism for the long-term stabilization of Earth's surface temperature. Journal of Geophysical Research 86, 9776–9782.

Wigley, T.M., Raper, S.C.B., 1987. Thermal expansion of sea water associated with global warming. Nature 330, 127–131.

Yamanaka, Y., Tajika, E., 1996. The role of the vertical fluxes of particulate organic matter and calcite in the oceanic carbon cycle: studies using an ocean biogeochemical general circulation model. Global Biogeochemical Cycles 10, 361–382.